Change of Internal Hydrogen Bonding of Methyl Red upon Photoisomerization Monitored by Forced Rayleigh Scattering

ARTICLE *in* THE JOURNAL OF PHYSICAL CHEMISTRY B · APRIL 1999

Impact Factor: 3.3 · DOI: 10.1021/jp9838442

5 AUTHORS, INCLUDING:

Kyung Seok Oh
SK Biopharmaceuticals
24 PUBLICATIONS **794** CITATIONS
SEE PROFILE

Kwang-Sun Kim
Korea University of Technology and Education
554 PUBLICATIONS **30,560** CITATIONS
SEE PROFILE

Taihyun Chang
Pohang University of Science and Technology
248 PUBLICATIONS **5,862** CITATIONS
SEE PROFILE

Daniel R. Spiegel
Trinity University
27 PUBLICATIONS **200** CITATIONS
SEE PROFILE

Change of Internal Hydrogen Bonding of Methyl Red upon Photoisomerization Monitored by Forced Rayleigh Scattering

Ha Seon Park, Kyung Seok Oh, Kwang S. Kim, and Taihyun Chang*,†

Department of Chemistry, POSTECH, Pohang, 790-784, Korea

Daniel R. Spiegel

Department of Physics, Trinity University, San Antonio, Texas 78212-7200

Received: September 24, 1998; In Final Form: January 15, 1999

A nonmonotonic, decay−growth−decay type forced Rayleigh scattering (FRS) decay profile was observed in the study of methyl red (o-MR) diffusion in polymer solutions in which the carboxylic hydrogen of o-MR can form a hydrogen bond with polymer chain segments (Lee and Lodge, *J. Phys. Chem.* **1987**, *91*, 5546; Lee et al. *Macromolecules* **1992**, *25*, 6977). The diffusivities of ground state o-MR (trans form) and of its photoexcited isomer (cis form) are different enough to show the nonmonotoic decay profile, but the origin of the behavior has not been fully understood. In order to elucidate this observation, the dependence of the decay profile shape on polymer concentration as well as on tempreature was investigated by FRS. From the results, we propose that the internal hydrogen-bonding strength between the carboxylic hydrogen and the azo nitrogen in o-MR changes upon photoisomerization from the trans to cis form, which results in the different diffusivities of the two isomers in hydrogen-bonding media. This proposition is supported by *ab initio* calculations on the molecular structure of o-MR.

Introduction

Hydrogen bonding plays an important role in a variety of physicochemical phenomena.[1] In many cases, intermolecular hydrogen bonding is of concern, but a large number of molecules have polar groups in positions that allow intramolecular hydrogen bonding. In certain circumstances, competition of intra- and intermolecular hydrogen bonding takes place,[2] which leads to intriguing observations. For example, we previously reported a diffusion study of methyl red in polymer solutions.[3] The diffusivity of methyl red was found to be significantly reduced if there exists hydrogen-bonding interaction between the dye and polymer chains such as poly(vinyl acetate) or poly(methyl methacrylate).[3−5] Furthermore, two structural isomers of methyl red (o-MR vs p-MR; the molecular structures of the two isomers are shown in the Experimental Section) showed a significantly different diffusivity in H-bonding media.[3,4] The diffusivity of p-MR was much lower than o-MR in H-bonding polymer solutions while these two isomers showed a similar diffusivity in non-H-bonding media. The difference was attributed to the internal H-bonding in o-MR between the carboxylic hydrogen and the azo nitrogen, which does not exist in p-MR. The internal H-bonding of the carboxylic hydrogen in turn weakened the external H-bonding of o-MR to the polymer chains.[3]

In addition, o-MR was found to show a nonmonotonic, decay−growth−decay (DGD) type decay profile in H-bonding media[3−8] while a normal single-exponential decay was found for p-MR as well as for the methyl ester of o-MR.[3] The DGD profile was not observed in polymer matrices which do not hydrogen bond with o-MR, e.g., polystyrene. The origin of the DGD profile has not been fully understood, although the profile indicates the diffusivities of ground state o-MR and of its photoproduct become different enough to exhibit the complementary grating effect[6,7,9−16] (assuming a reasonable value for the refractive index contrast between the complementary gratings of methyl red, as discussed below). In this paper, we demonstrate that the difference in internal hydrogen-bonding strength of o-MR in its two photoisomeric states (i.e., cis and trans form) is responsible for the nonmonotonic decay profile.

Forced Rayleigh Scattering. Forced Rayleigh scattering is a transient optical grating technique which utilizes a spatial concentration modulation of the photochemical probes as a diffraction grating.[17−19] The concentration modulation is generated by a brief exposure of the sample containing probe molecules to a periodic pattern of light intensity (writing process). Upon exposure, the probe molecules undergo a photochemical reaction and make a periodic modulation in the concentration of the photoreaction product. If the photoproduct of the probe molecule has a refractive index (phase grating) or absorptivity (amplitude grating) that differs from the original state, the concentration modulation can act as an optical diffraction grating. Observing the decay of the diffracted light (reading process), one can measure the relaxation rate of the concentration modulation, which contains information on the diffusivity of the probe molecules in various systems (simple liquids,[20] porous media,[21,22] liquid crystals,[23,24] polymer solutions, melts and glasses[3−5,9,11,12,16,25−28] including block copolymer systems,[29,30] supercooled liquids,[31,32] and magnetic fluids[33]). FRS can also be used to study electrophoretic mobility,[34,35] lifetime of the photoproduct,[36,37] subsequent photochemical reactions,[38,39] polymer polydispersity[40] by thermal diffusion,[41,42] near-surface diffusion using evanescent wave,[43] and so on. In this study, our discussion is restricted to the mass diffusion process, which can be realized by choosing a probe that relaxes

† Tel: +82-562-279-2109. Fax: +82-562-279-3399. Email: tc@postech.ac.kr.

10.1021/jp9838442 CCC: $18.00
Published on Web 03/16/1999

back to its original state with a sufficiently long photoproduct lifetime and no subsequent photochemical reactions.

The transient concentration grating formed by the writing process is in fact a composite of two complementary gratings of the excess ground state probe and of its photoproduct, which are 180° out of phase.[10,13,18] Therefore, the FRS decay profile of a phase grating follows the following model function[6,7,9−14]

$$I_d(t) = [A_1 \exp(-t/\tau_1) - A_2 \exp(-t/\tau_2) + B_{coh}]^2 + B_{inc} \quad (1)$$

where τ_1 and τ_2 are the respective decay time constants of two complementary gratings, A_1 and A_2 represent the amplitudes of the optical fields diffracted from each complementary phase grating, and B_{coh} and B_{inc} are the coherent and incoherent background, respectively. The decay time constant τ is a function of the probe diffusivity and the lifetime of the photoproduct so that information on the dynamics of the probe can be obtained. If the relaxation rates of two complementary gratings are the same, the FRS signal shows a single-exponential decay.

$$I_d(t) = [A \exp(-t/\tau) + B_{coh}]^2 + B_{inc} \quad (2)$$

Experimental Section

The probe dyes, 2-[4′-(dimethylamino)phenylazo]benzoic acid (methyl red, o-MR) and 4-[4′-(dimethylamino)phenylazo] benzoic acid (p-MR), were acquired from Aldrich and TCI, respectively, and used without further purification. The methyl

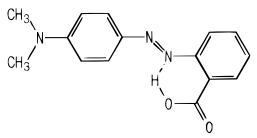

o-MR

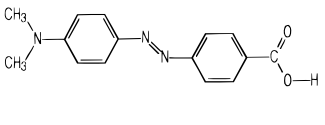

p-MR

ester of p-MR (CH_3-p-MR) was prepared through reaction with methyl alcohol in the presence of sulfuric acid as a catalyst. The methyl ester of o-MR (CH_3-o-MR) was synthesized through reaction with methyl alcohol after acylation of o-MR with $SOCl_2$. Poly(vinyl acetate) (PVAc) was obtained from Aldrich and its M_w and M_w/M_n were determined by gel permeation chromatography as 87,000 and 2.4 relative to polystyrene standards, respectively.

Toluene solutions of polymer and probe dye were prepared gravimetrically, and the polymer concentration is represented by the volume fraction calculated from the density of PVAc and toluene at 25 °C. The probe dye concentration was kept at 0.1 mg/mL. We experimentally confirmed that there was no dye concentration dependence of the dye diffusivity and FRS decay profile in this concentration range. The solutions were filtered through 0.2 μm pore PTFE membrane filters (Gelman) directly to a 5 mm path length spectroscopic quartz cuvette for the FRS measurements.

The FRS apparatus used in this study was described in detail elsewhere.[44] In order to eliminate the contribution of B_{coh}, we inserted an optical glass window into the path of one of the two writing beams (crossing at the sample to generate an optical grating) for every other pulse during the accumulation of the FRS signal. The tilt angle of the window was adjusted to retard the phase of the laser beam so that it shifts the optical grating by a half of its period. This adjustment was done visually by monitoring the grating projected on a distant screen by use of a short focal length convex lens. The phase shift of the optical grating results in a phase shift of the diffracted optical field by π. Accumulation of the diffracted intensity from the grating

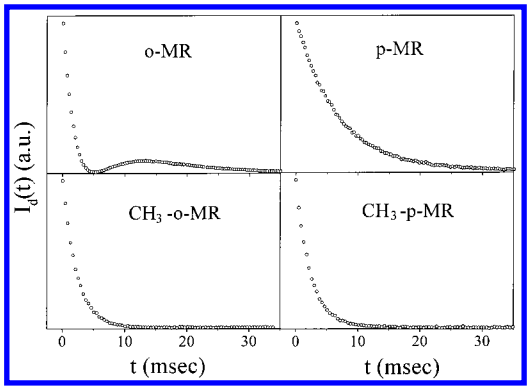

Figure 1. FRS decay profiles of o-MR, p-MR, and their methyl esters in 10% PVAc/toluene solution at a grating spacing of 12.1 μm. o-MR shows a unique nonmonotonic decay profile while the other three dyes show good single-exponential decay profiles.

phase shifted by π every other pulse eliminates B_{coh} in eqs 1 and 2.[45] The 488 nm line of an Ar ion laser (Coherent, Model 90-3) is used for the writing beam and the 632.8 nm line of a He/Ne laser (Melles Griot, 5 mW) for the reading beam. The temperature of the cell was controlled better than ± 0.1 °C.

Since methyl red does not absorb the reading beam, the transient diffraction grating created in the sample cell is the phase grating and we used eqs 1 and 2 for the analysis of the FRS decay profile. The analysis scheme for the decay profiles depended on the shape of the signal. For single-exponentially decaying signals, nonlinear regression fit to eq 2 (without B_{coh}) was used. For decay−growth−decay (DGD) type decay profiles, it was not possible to obtain a unique result by fitting to eq 1. It is well-known that a unique multiparameter fit is not possible when the difference between τ_1 and τ_2 is not large,[3−5,9,11−16] although multiparameter fitting or the stripping analysis method was practiced when the difference between τ_1 and τ_2 was large enough.[6,7,34] Instead, the mean decay time constant was determined by the Δt method (Δt, time lapse between the dip and maximum position).[14] When the difference between τ_1 and τ_2 is small, Δt is an excellent approximation to the mean decay time constant. Then the diffusivity of MR is obtained from the slope of $1/\tau$ (single-exponential decay) or $1/\Delta t$ (DGD type decay) vs q^2 plot, where $q = 2\pi/d$ and d is the spacing of the optical grating created by crossing the writing beams at the sample.

Results and Discussion

Decay-Growth-Decay Profile. FRS decay profiles with four probe dyes, o-MR, p-MR, and their methyl esters (CH_3-o-MR and CH_3-p-MR) in 10% PVAc/toluene solution, are displayed in Figure 1. They are measured at an identical grating spacing of 12.1 μm. A nonmonotonic decay is distinct for o-MR, while the other dyes exhibit single-exponential decay profiles. p-MR shows a slower decay than CH_3-o-MR or CH_3-p-MR due to the H-bonding between p-MR and PVAc.[3,4] The nonmonotonic decay profile of o-MR is unique among the four dyes in PVAc/toluene solution. In non-H-bonding media, such as either pure toluene or polystyrene (PS)/toluene solution, all four dyes including o-MR show single-exponential decay profiles. Their decay profile shapes and the mean diffusivities determined by Δt method are summarized in Table 1. We note that the diffusivities of the four dyes are very close in pure solvent (toluene) and in a medium in which the probe dye does not hydrogen bond to the polymer chains (PS/toluene solution). This indicates that the hydrodynamic sizes of the four dyes are similar. However, the diffusivities in PVAc/toluene solution

TABLE 1: FRS Decay Profile Shapes and Diffusivities ($\times 10^{-6}$ cm^2/s) of o-MR, p-MR, and Their Methyl Esters in Three Different Media at 25 °C[a]

probe	toluene	10% PS/toluene	10% PVAc/toluene
o-MR	SE, 12.7 ± 0.2	SE, 8.8 ± 0.3	DGD, 4.4 ± 0.2
CH_3-o-MR	SE, 12.0 ± 0.2	SE, 8.0 ± 0.1	SE, 7.9 ± 0.2
p-MR	SE, 12.0 ± 0.2	SE, 8.1 ± 0.2	SE, 2.7 ± 0.2
CH_3-p-MR	SE, 12.8 ± 0.6	SE, 8.3 ± 0.3	SE, 8.4 ± 0.4

[a] SE: single-exponential decay. DGD: decay−growth−decay.

differ from one another significantly. The H-bonding interaction between the acid form of methyl red (o-MR or p-MR) and PVAc chain retards the diffusion of the dyes significantly, while their methyl esters do not show a significant change. Diffusion of o-MR is less retarded than p-MR due to the internal H-bonding in o-MR, which in turn weakens the external H-bonding with PVAc.[3] Also, a nonmonotonic DGD type decay profile is observed only for o-MR and only when H-bonding interaction exists between the dye and the polymer chain such as in PVAc or poly(methyl methacrylate) (PMMA) solution.[3−5,44] Therefore, the origin of the DGD type decay profile found for o-MR is closely related to the dye's H-bonding to the polymer chains.

The DGD profile found for o-MR demonstrates that two complementary gratings, which consist of excess trans and cis isomers of the dye in the concentration modulation, decay at different rates.[6,7] Since the refractive index of trans form is known to be larger than that of the cis isomer, and the refractive indices of both isomers are larger than that of the background (PVAc/toluene solution), the diffraction efficiency of the trans isomer rich grating is higher than the cis form rich grating ($A_{trans} > A_{cis}$).[13,46] In this circumstance, the relaxation rate of the concentration grating (i.e., the diffusivity of o-MR) should be higher for the trans-rich grating than for the cis-rich grating in order to show a DGD type signal ($\tau_{trans} < \tau_{cis}$).[3,11−13] If the trans isomer has a lower diffusivity than the cis isomer, a different type of decay profile (growth decay or non-single-exponential monotonic decay) would be observed instead of the DGD type profile.[9,11,13] Wang and co-workers also found a lower diffusivity of cis o-MR relative to its trans form in poly(ethylene glycol) and poly(caprolactone) diol. They interpreted the observation as due to a stronger interaction between the cis form and the polymer host without suggesting the nature of the interaction.[6,7] Here we propose that the higher diffusivity of the trans form relative to the cis form of o-MR in hydrogen-bonding media arises from the difference in internal H-bonding strength between two isomers.

PVAc Concentration Dependence. In Figure 2, FRS decay profiles of o-MR at three different concentrations (3.0%, 4.8%, and 10.0%) of PVAc/toluene solutions are displayed. They are both measured at the same grating spacing of 12.1 μm and at a temperature of 25.0 °C. The signal is normalized to the initial signal intensity for visual aid. Judging from the position of the dip and maximum, the signal decays more slowly at higher PVAc concentration. It indicates that the diffusion of o-MR is retarded with PVAc concentration. In addition, it is evident that the relative intensity at the maximum grows as the concentration of PVAc is increased. For an easier comparison of the profile shapes, in Figure 3 the abscissa is normalized by Δt, which is a fairly good approximation to the mean decay time constant of the two complementary gratings.[14,15] It is clear that, as the PVAc concentration increases, $t_{dip}/\Delta t$ becomes shorter and the signal intensity at the maximum increases. A simple derivation using eq 1 leads to the following formula:

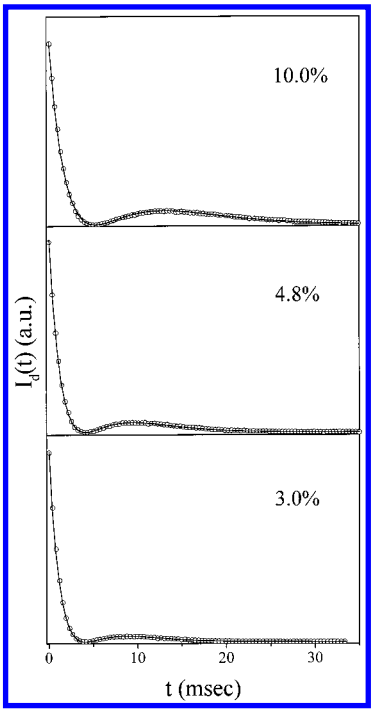

Figure 2. FRS decay profiles of o-MR at three different PVAc concentrations (from top, 10.0%, 4.8%, and 3.0%) at 25 °C. The grating spacing is 12.1 μm. The ordinate is normalized to the initial amplitude for visual aid. The solid lines represent the fit according to eq 1.

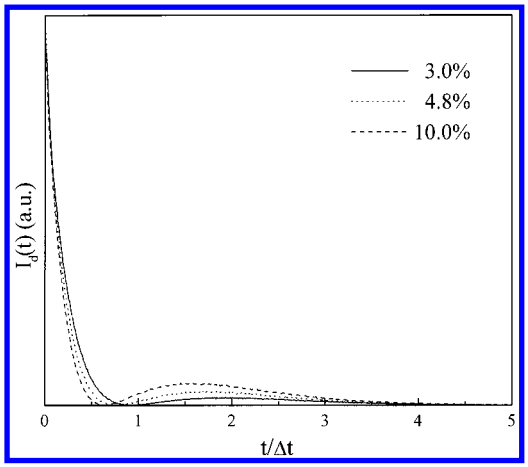

Figure 3. The same three FRS decay profiles of o-MR as in Figure 2 displayed with the abscissa normalized to the mean decay time constants ($\Delta t = t_{max} - t_{dip}$) so that the relative shapes can be easily compared: dashed line, 10.0%; dotted line, 4.8%; solid line, 3.0%. It is clear that the signal intensity at the maximum increases and $t_{dip}/\Delta t$ becomes shorter as the PVAc concentration increases, which indicates that τ_{cis}/τ_{trans} increases.

$$\frac{t_{dip}}{\Delta t} = \frac{\ln(A_{trans}/A_{cis})}{\ln(\tau_{cis}/\tau_{trans})} \qquad (3)$$

where B_{coh} was neglected since it was experimentally eliminated in this study. Therefore, the trend observed in Figure 3 indicates that two decay time constants get further apart (τ_{cis}/τ_{trans} increases) as the PVAc concentration is increased, provided the contrast of the complementary gratings (A_{trans}/A_{cis} in eq 3) remains constant. This proviso is reasonable in this system because the FRS signal of o-MR is due mainly to the refractive index contrast (phase grating) when the reading beam wavelength is 632.8 nm,[13] and the change of PVAc concentration does not significantly alter the refractive index of the background due to the similar refractive indices of PVAc and toluene.[46,47]

TABLE 2: Decay Time Constants of Complementary Gratings at 25 °C in PVAc/Toluene Solutions at Three Different Concentrations

PVAc (%)	τ_{cis}/τ_{trans}	Δt (ms)	D ($\times 10^{-6}$ cm^2/s)
3.0	1.14	4.77	7.7 ± 0.6
4.8	1.16	5.87	6.6 ± 0.3
10.0	1.18	8.63	4.4 ± 0.2

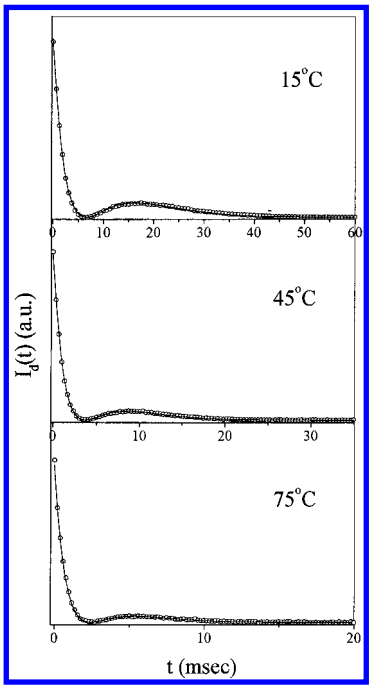

Figure 4. FRS decay profiles of o-MR in 10% PVAc/toluene solution at three different temperatures (from top, 15, 45, and 75 °C). The grating spacing is 12.1 μm. The ordinate is normalized to the initial signal amplitude for visual aid. The solid lines represent the fit according to eq 1.

These decay profiles are fitted to eq 1 by a nonlinear regression method and the solid lines in Figure 2 represent the fit results. For the fitting, the contrast of A_{trans}/A_{cis} was fixed at 9.4/8.4 using the estimated refractive index of the azo dye in the system.[13] The quality of the fit appears good and the fit results are summarized in Table 2. The ratio of τ_{cis}/τ_{trans} progressively increases with the concentration of PVAc. In other words, the difference in the diffusivity between the cis and trans isomers becomes larger as the concentration of the H-bond acceptor (PVAc) increases, which makes the DGD type decay signal more and more pronounced as displayed in Figures 2 and 3. Thus, the observation displayed in Figures 2 and 3 and Table 2 is consistent with the hypothesis that the trans and cis isomers of o-MR make hydrogen bonds of different strength with PVAc; the trans isomer appears to form a weaker external H-bond with PVAc chains compared to the cis isomer.

Temperature Dependence and the Origin of DGD Profile. FRS decay profiles of o-MR at three different temperatures (15, 45, and 75 °C) are displayed in Figure 4. They are measured at the same grating spacing as Figure 2 and at a fixed concentration of 10% PVAc/toluene solution. The ordinate is again normalized for visual aid. In Figure 5 the abscissa is also normalized to Δt. These profiles exhibit essentially the same trend as observed in PVAc concentration dependence shown in Figure 2. These decay profiles are fitted to eq 1 by a nonlinear regression method keeping A_{trans}/A_{cis} constant at 9.4/8.4. The solid lines in Figure 4 represent the fit results and the fit results are summarized in Table 3. It is clear that the difference between τ_{trans} and τ_{cis} becomes smaller as the temperature increases. This is again

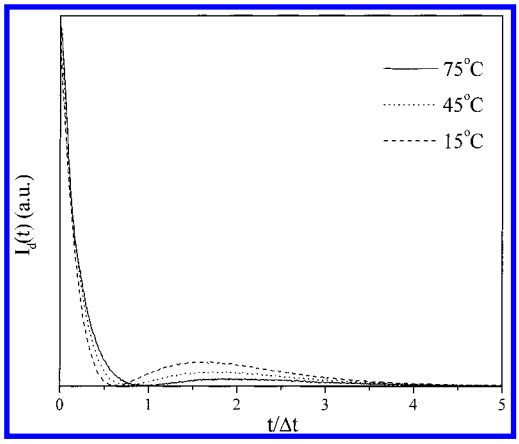

Figure 5. The same three FRS decay profiles of o-MR as in Figure 4: dashed line, 15 °C; dotted line, 45 °C; solid line, 75 °C. The abscissa is normalized to the mean decay time constants (Δt) so that relative shape, can be easily compared. It is clear that as the temperature is decreased, the signal intensity at the maximum increases and $t_{dip}/\Delta t$ becomes shorter, which indicates that τ_{cis}/τ_{trans} increases.

TABLE 3: Decay Time Constants of Complementary Gratings in 10% PVAc/Toluene Solutions at Three Different Temperatures

temp (°C)	τ_{cis}/τ_{trans}	Δt (ms)	D ($\times 10^{-6}$ cm^2/s)
15	1.18	10.74	3.4 ± 0.1
45	1.16	5.26	7.3 ± 0.2
75	1.15	2.93	12.7 ± 0.8

consistent with the hypothesis that H-bonding is responsible for the difference between τ_{trans} and τ_{cis} since H-bonding becomes weaker as the temperature increases.[48]

Putting these experimental observations together, we propose the following for the origin of the DGD type signal. In general, the trans isomer of an azobenzene derivative is known to have a coplanar structure of two phenyl rings and the azo group.[49,50] In the cis isomer, however, the two phenyl rings are twisted out of the plane of the azo group due to the steric hindrance between phenyl hydrogens.[49,50] This effect is observed spectroscopically, such that consequent reduction of delocalization of π electrons results in the hypochromic effect and the hypsochromic shift of the $\pi-\pi^*$ transition band.[49,50] Since the coplanar structure of the phenyl rings and the azo group is expected to be favorable for the internal H-bonding formation of o-MR via six-membered ring conformation, the internal H-bonding in the trans form of o-MR would be stronger, which in turn weakens the external H-bonding with PVAc backbone more compared to the cis isomer. This leads to a larger reduction in the diffusivity of the cis isomer relative to the trans form, which results in a DGD type decay for o-MR in H-bonding environments. This hypothesis is consistent with the fact that such a DGD signal is observed only for o-MR, not for its methyl ester or p-MR, and only in polymer solutions which interact with o-MR via H-bonding, such as PVAc or PMMA. From the results we can also note that a small change of decay time constants, a few % as shown in Tables 2 and 3, can alter the shape of decay profile substantially, as displayed in Figures 3 and 5. This is an expected result when complementary gratings play a role.[13]

Ab Initio Calculations. It has been proposed above, based on the experimental results reported, that the strength of the internal hydrogen bonding between the carboxylic hydrogen and the azo nitrogen in o-MR changes upon photoisomerization between cis and trans forms, resulting in different diffusivities. To further test this proposal, we performed an ab initio

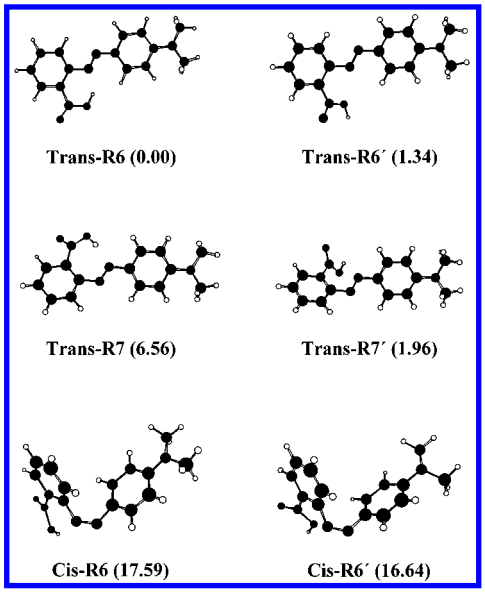

Figure 6. Structures and relative energies of conformers of o-MR. The left insets are conformers with internal hydrogen bonding, while the right insets (with primes in their codes) are conformers without internal hydrogen bonding. The relative energies (kcal/mol) in parentheses were obtained by HF/6-31G*.

conformational study of o-MR. We investigated the possible conformers of the cis and trans isomers of o-MR with and without internal hydrogen bonding between the carboxylic hydrogen and the azo nitrogen. There are two trans conformers with internal hydrogen bonding forming six- and seven-membered rings (Trans-R6, Trans-R7), and one cis isomer with internal hydrogen bonding forming a six-membered ring (Cis-R6). In addition, there are three corresponding conformers without internal hydrogen bonding (Trans-R6′, Trans-R7′, Cis-R6′). Here the primes denote the cases of non-hydrogen-bonded virtual rings. All the conformers were fully optimized by Hartree−Fock (HF) theory with GAMESS[51] using the 6-31G* basis set. Structures and relative energies are shown in Figure 6. In the trans isomers, Trans-R6 is the lowest energy conformer, followed by Trans-R6′, Trans-R7′, and Trans-R7. The predicted relative energies of Trans-R6′, Trans-R7′, and Trans-R7 with respect to Trans-R6 are 1.34, 1.96, and 6.56 kcal/mol, respectively. For the cis isomers, Cis-R6 is slightly higher in energy than Cis-R6′ by 0.95 kcal/mol. The predicted relative energies of Cis-R6′ and Cis-R6 with respect to Trans-R6 are 16.64 and 17.59 kcal/mol, respectively. The conformational stability can be understood in terms of molecular structure, in particular the internal hydrogen bond. Conformers of the trans isomer have a planar structure (with only a small distortion to reduce the electron repulsion between the carboxylic group and the azo group). Conformers with internal hydrogen bonding are expected to be more stable than conformers without internal hydrogen bonding. Trans-R6 is highly stabilized by an internal hydrogen bond whose distance is 1.831 Å in the six-member ring conformation. Trans-R7 also has an internal hydrogen bond whose distance is 1.807 Å in the seven-membered ring conformation. The strain of the seven-membered ring, however, causes Trans-R7 to be less stable than Trans-R6 as well as the conformers without internal hydrogen bonding. In the cis isomers, the phenyl rings are twisted out of the plane of the azo group due to the steric hindrance between phenyl hydrogen atoms. Cis-R6 has an internal hydrogen bond whose distance is 1.916 Å. However, the orientation required for internal hydrogen bonding is not favorable, making Cis-R6 less stable than Cis-R6′. These results indicate that, owing to the strong internal hydrogen bonding, Trans-R6 is the most stable conformer among the trans isomers, while Cis-R6′ is more stable than Cis-R6 for the cis isomers. This is in full agreement with our experimental findings.

In summary, we have studied the temperature and polymer concentration dependence of the tracer diffusion of methyl red derivatives in polymer solutions by FRS. From the diffusivity results and FRS decay profile shapes, we found that hydrogen bonding between o-MR and PVAc is responsible not only for the retarded diffusion but also for the decay−growth−decay FRS signal of o-MR. We proposed that the nonmonotonic decay is caused by internal hydrogen bonding in o-MR. Molecular structures of trans and cis isomers of o-MR obtained by ab initio calculations support this proposition.

Acknowledgment. This study was supported in part by the Basic Science Research Institute Program, Ministry of Education (BSRI-97-3438). We thank Jae Young Lee and Jungmoon Sung for the help in the FRS experiments. It is also acknowledged that most of the calculations were performed using Cray C90 and T3E at SERI. D.R.S. gratefully acknowledges support from the National Science Foundation (Grant No. CHE-9711426).

References and Notes

(1) Pimental, G. C.; McClellan, A. L. *The Hydrogen Bond*; W. H. Freeman and Co.: San Francisco, 1960.
(2) Nagy, P. I.; Durant, G. J.; Smith, D. A. *Modeling the hydrogen bond*; ACS Symp. Ser. 569; Smith, D. A., Ed.; American Chemical Society: Washington, DC, 1994.
(3) Lee, J.; Park, K.; Chang, T.; Jung, J. C. *Macromolecules* **1992**, *25*, 6977.
(4) Park, H. S.; Sung, J.; Chang, T. *Macromolecules* **1996**, *29*, 3216.
(5) Lee, J. A.; Lodge, T. P. *J. Phys. Chem.* **1987**, *91*, 5546.
(6) Xia, J. L.; Gong, S. S.; Wang, C. H. *J. Phys. Chem.* **1987**, *91*, 5805.
(7) Xia, J. L.; Wang, C. H. *J. Chem. Phys.* **1988**, *88*, 5211.
(8) Lodge, T. P.; Lee, J. A.; Frick, T. S. *J. Polym. Sci. B.* **1990**, *28*, 2607.
(9) Huang, W. J.; Frick, T. S.; Landry, M. R.; Lee, J. A.; Lodge, T. P.; Tirrell, M. *AIChE J.* **1987**, *33*, 573.
(10) Johnson, C. S. Jr. *J. Opt. Soc. Am. B* **1985**, *2*, 317.
(11) Spiegel, D. R.; Sprinkle, M. B.; Chang, T. *J. Chem. Phys.* **1996**, *104*, 4920.
(12) Chapman, B. R.; Gochanour, C. R.; Paulaitis, M. E. *Macromolecules* **1996**, *29*, 5635.
(13) Park, S.; Sung, J.; Kim, H.; Chang, T. *J. Phys. Chem.* **1991**, *95*, 7121.
(14) Park, S.; Yu, H.; Chang, T. *Macromolecules* **1993**, *26*, 3086.
(15) Park, H. S.; Sung, J.; Lee, H.; Chang, T.; Spiegel, D. R. *Bull. Korean Chem. Soc.* **1997**, *18*, 1006.
(16) Spiegel, D. R.; Marshall, A. H.; Jukam, N. T.; Park, H. S.; Chang, T. *J. Chem. Phys.* **1998**, *109*, 267.
(17) Eichler, H. J.; Gunter, P.; Pohl, D. W. *Laser-Induced Dynamic Gratings*; Springer: Berlin, 1986
(18) Nelson, K. A.; Casalegno, R.; Dwayne Miller, R. J.; Fayer, M. D. *J. Chem. Phys.* **1982**, *77*, 1144.
(19) Lodge, T.; Chapman, B. *Trends Polym.* **1997**, *5*, 122.
(20) Terazima, M.; Okamoto, K.; Hirota, N. *J. Phys. Chem.* **1993**, *97*, 5188.
(21) Drake, J. M.; Klafter, J. *Phys. Today* **1990**, *43*, 46.
(22) Guo, Y.; O'Donohue, S. J.; Langley, K. H.; Karasz, F. E. *Phys. Rev. A* **1992**, *46*, 3335.
(23) Hervert, H.; Urbach, W.; Rondelez, F. *J. Chem. Phys.* **1978**, *68*, 2725.
(24) Moriyama, T.; Takanishi, Y.; Ishikawa, K.; Takezoe, H.; Fukuda, A. *Liq. Cryst.* **1995**, *18*, 639.
(25) Hervert, H.; Léger, L.; Rondelez, F. *Phys. Rev. Lett.* **1979**, *42*, 1681.
(26) Wang, C. H.; Xia, J. L.; Yu, L. *Macromolecules* **1991**, *24*, 3638.
(27) Ehlich, D.; Sillescu, H. *Macromolecules* **1990**, *23*, 1600.
(28) Xia, J.; Wang, C. H. *J. Polym. Sci. B* **1995**, *33*, 899.
(29) Zielinski, J. M.; Heuberger, G.; Sillescu, H.; Wiesner, U.; Heuer, A.; Zhang, Y.; Spiess, H. W. *Macromolecules* **1995**, *28*, 8287.
(30) Lodge, T. P.; Dalvi, M. C. *Phys. Rev. Lett.* **1995**, *75*, 657.
(31) Heuberger, G.; Sillescu, H. *J. Phys. Chem.* **1996**, *100*, 15255.

(32) Köhler, W.; Fytas, G.; Steffen, W.; Reinhardt, L. *J. Chem. Phys.* **1996**, *104*, 248.
(33) Bacri, J. C.; Cebers, A.; Bourdon, A.; Demouchy, G.; Heegaard, B. M.; Perzynski, R. *Phys. Rev. Lett.* **1995**, *74*, 5032.
(34) Rhee, K. W.; Shibata, T.; Barish, A.; Gabriel, D. A.; Johnson, C. S. Jr. *J. Phys. Chem.* **1984**, *88*, 3944.
(35) Kim, H.; Chang, T.; Yu, H. *J. Phys. Chem.* **1984**, *88*, 3946.
(36) Chang, T.; Kim, H.; Yu, H. *Chem. Phys. Lett.* **1984**, *111*, 64.
(37) Wang, C. H.; Xia, J. L. *J. Phys. Chem.* **1992**, *96*, 190.
(38) Deeg, F. W.; Pinsl, J.; Bräuchle, Chr. *J. Phys. Chem.* **1986**, *90*, 5710.
(39) Hara, T.; Hirota, N.; Terazima, M. *J. Phys. Chem.* **1996**, *100*, 10194.
(40) Rossmanith, P.; Köhler, W. *Macromolecules* **1996**, *29*, 3203.
(41) Köhler, W. *J. Chem. Phys.* **1993**, *98*, 660.
(42) Köhler, W.; Rosenauer, C.; Rossmanith, P. *Int. J. Thermophys.* **1995**, *16*, 11.
(43) Sainov, S. *J. Chem. Phys.* **1996**, *104*, 6901.
(44) Lee, J.; Park, T.; Sung, J.; Park, S.; Chang, T. *Bull. Korean Chem. Soc.* **1991**, *12*, 569.
(45) Miles, D. G. Jr.; Lamb, P. D.; Rhee, K. W.; Johnson, C. S. Jr. *J. Phys. Chem.* **1983**, *87*, 4815.
(46) Weast, R. C., Ed. *Handbook of Chemistry and Physics*, 70th ed.; CRC Press: Boca Raton, FL; 1989.
(47) Brandrup, J., Immergut, E. H., Eds., *Polymer Handbook*, 3rd ed.; John Wiley & Sons: New York, 1989.
(48) Sung, J.; Chang, T. *Polymer* **1993**, *34*, 3741.
(49) Brown, G. H., Ed., *Photochromism*; Wiley-Interscience: New York, 1971.
(50) Dürr, H., Bouas-Laurent, H., Eds., *Photochromism*; Elsevier: New York, 1990.
(51) Schmit, M. W.; Baldridge, K. K.; Boatz, J. A.; Elbert, S. T.; Gordon, M. S.; Jensen, J. H.; Koseki, S.; Matsunaga, N.; Nguyen, K. A.; Su, S.; Windus, T. L. *J. Comput. Chem.* **1993**, *14*, 1347.